



HAL
open science

Variability of ambient particulate matter loading at Henties Bay, Namibia

Monray Belelie, Henno Havenga, Danitza Klopper, Rebecca Garland, Brigitte Language, Paola Formenti, Andreas Namwoonde, Roelof Burger, Stuart Piketh

► **To cite this version:**

Monray Belelie, Henno Havenga, Danitza Klopper, Rebecca Garland, Brigitte Language, et al.. Variability of ambient particulate matter loading at Henties Bay, Namibia. *The Clean Air Journal*, 2023, 33 (2), 10.17159/caj/2023/33/2.16670 . hal-04568698

HAL Id: hal-04568698

<https://hal.science/hal-04568698>

Submitted on 6 May 2024

HAL is a multi-disciplinary open access archive for the deposit and dissemination of scientific research documents, whether they are published or not. The documents may come from teaching and research institutions in France or abroad, or from public or private research centers.

L'archive ouverte pluridisciplinaire **HAL**, est destinée au dépôt et à la diffusion de documents scientifiques de niveau recherche, publiés ou non, émanant des établissements d'enseignement et de recherche français ou étrangers, des laboratoires publics ou privés.



Distributed under a Creative Commons Attribution 4.0 International License

Research article

Variability of ambient particulate matter loading at Henties Bay, Namibia

Monray D Belelie^{1*}, Henno Havenga¹, Danitza Klopper², Rebecca M Garland^{3,4}, Brigitte Language^{1,5}, Paola Formenti⁵, Andreas Namwoonde⁶, Roelof P Burger¹, and Stuart J Piketh¹

¹Unit for Environmental Sciences and Management, North-West University, Potchefstroom, South Africa

²Department of Geography and Environmental Sciences, School of Agricultural and Environmental Sciences, University of Limpopo, Mankweng

³Smart Places, Council for Scientific and Industrial Research, Pretoria, South Africa

⁴Department of Geography, Geo-informatics and Meteorology, University of Pretoria, Pretoria, South Africa

⁵Laboratoire Interuniversitaire des Systèmes Atmosphériques (LISA), UMR CNRS, Université Paris-Est Créteil, Université de Paris, Institut Pierre Simon Laplace, Créteil, France

⁶Sam Nujoma Marine and Coastal Resources Research Centre, Sam Nujoma Campus, University of Namibia, Henties Bay, Namibia
Corresponding author: monraybelelie@gmail.com

Received: 14 August 2023 - Reviewed: 3 October 2023 - Accepted: 5 October 2023

<https://doi.org/10.17159/caj/2023/33/2.16670>

Abstract

The Namibian coast is one of the areas of international interest for aerosol studies. This is due to the region's importance for the global radiation budget because of the presence of a semi-permanent stratocumulus cloud along the coast. Aerosol particles may scatter/absorb radiation and directly influence how long clouds last by modifying their properties. This is all dependent on the particles' chemical and physical properties influenced by the sources they were emitted from. In this study, we identified and investigated episodes of high (HAE) and low (LAE) PM concentrations and the meteorology that may favour their occurrence. Here, we investigated PM_{2.5} (particles with an aerodynamic diameter of 2.5 µm or less) and PM₁₀ (particles with an aerodynamic diameter of 10 µm or less) at Henties Bay, Namibia. Daily aerosol measurements were taken with E-samplers between 15 and 29 July 2019. The Hybrid Single-Particle Lagrangian Integrated Trajectory (HYSPLIT) model was used to investigate the long-range atmospheric transport of air masses that reached Henties Bay. The study found that during HAEs, the average PM_{2.5} concentration was 28.40 ± 18.10 µg/m³ and the average PM₁₀ concentration was 68.20 ± 44.3 µg/m³. In contrast, during LAEs, the average PM_{2.5} concentration was 13.3 ± 9.52 µg/m³ and the average PM₁₀ concentration was 30.00 ± 23.00 µg/m³. In both fractions, there was an observed dominant contribution from marine sources.

Keywords

PM, stratocumulus cloud, HYSPLIT, HAEs, LAEs

Introduction

Ambient particulate matter (PM) is used as an air quality indicator (Chen & Hoek, 2020) and has impacts on phenomena such as haze formation and climate change (Liu et al., 2018). PM is commonly categorised based on its size as PM_{2.5} (aerosol with an aerodynamic diameter of 2.5 µm or less) and PM₁₀ (aerosol with an aerodynamic diameter of 10 µm or less) (Kastury et al., 2017; Kastury et al., 2018). The distribution and physicochemical properties of PM particles in the atmosphere vary horizontally and vertically. This is due to their uneven source distribution and short lifetime, which is typically less than 10 days for particles <1 µm and even shorter for particles >1 µm (Klopper et al., 2020). A variety of primary sources, both natural and anthropogenic, may

emit PM. It can also be formed as secondary particles through photochemical processes involving the primary precursors (Dai et al., 2019; Zalakeviciute et al., 2020; Khan et al., 2021). These sources include biomass burning, road traffic, sea salt, and dust, amongst others (Squizzato et al., 2017; Zalakeviciute et al., 2020; Psistaki et al., 2023). Given the various possible sources, the PM concentration and composition at a site depend on several factors such as the regional background and its meteorology (Yang et al., 2020; Zalakeviciute et al., 2020).

The Namibian coast is one of the areas of interest for PM studies and their impact on the climate. A recent study found that Namibian coastal areas have predominant PM inputs from sea

salt (75%) and mineral dust (16%) (Klopper et al., 2020). The production of primary marine aerosols is largely influenced by local wind stress, with pure sea salt being the major constituent. This production yields marine particles with a diameter of <20 μm ranging from 2000 to 10000 T/yr (de Leeuw et al., 2011; Fuzzi et al., 2015). Ultra-fine marine particles (<1 μm) may be transported over long atmospheric distances while the larger particles are deposited close to where they were produced (Fuzzi et al., 2015). The local meteorology in the arid region is influenced by the adjacent cold Benguela ocean current and semi-permanent stratocumulus cloud layer. The Benguela region is known for its high marine biogenic productivity which emits sulphur-containing compounds such as dimethyl sulphide and hydrogen sulphide into the surrounding atmosphere (Klopper et al., 2020). Once in the atmosphere, these compounds may be oxidised and produce secondary particles which then contribute to cloud droplet formation of the stratocumulus cloud (Andreae et al., 1995).

Anthropologically induced land surfaces, desert regions, and ephemeral dry lakes or riverbeds are the primary sources of dust globally (Mahowald et al., 2009). Specifically, most of its budget originates from fluvial dust sources (Poulton & Raiswell, 2002). Dry ephemeral lakes found in arid and semi-arid localities, such as Makgadikgadi and Etosha pans in Southern Africa, are the major global sources of aeolian dust to the ocean (Prospero et al., 2002). These sources have been hypothesised to be significant for fertilising the adjacent ocean (Piketh et al., 2000). Other important Southern African dust sources are the Kuiseb, Huab, Tsauchab, and Omaruru ephemeral riverbeds in Namibia. They may also play a noteworthy fertilisation role in phytoplankton in the adjacent Benguela (Jacobson et al., 2000; Jacobson & Jacobson, 2013; Dansie et al., 2017). Analyses using remote sensing have also revealed that these riverbeds are significant sources of dust plumes transported to the southern Atlantic (Eckardt & Kuring, 2005; Vickery et al. 2013).

The Henties Bay Aerosol Observatory (HBAO) continuously monitors aerosol measurements, including their chemical composition and concentrations (Klopper et al., 2020). This study expands on previous research at the HBAO by identifying coastal episodes of high and low PM concentrations, and the weather conditions that favour the occurrence of these episodes.

Methods

Sampling

Concentrations of particulate matter (PM) were sampled at the University of Namibia's Sam Nujoma campus (S22°5'43.944"; E14°15'9552") between 15 and 29 July 2019 (Figure 1) (Figure 2). The campus is located next to the Omaruru riverbed, southwest of the Etosha Pan and Huab riverbed and northwest of the Kuiseb- and Tsauchab riverbeds. The sampling was done by concurrently operating two E-samplers mounted on tripods (Met One Instrument, 2011). The E-samplers have a particle size range of 0.1–100 μm and a measurement range between 0 and 65 $\mu\text{g}/\text{m}^3$

m^3 with a precision of 2%. The measurements were converted from mg/m^3 to $\mu\text{g}/\text{m}^3$ by multiplying each value by 1000. One sampler continuously measured $\text{PM}_{2.5}$ and the other measured PM_{10} (Figure 2). Measurements were taken in 15-minute intervals at a flow rate of 2 L/min.

Unfortunately, the meteorology during the sampling period was not measured at the site. However, the Wlotzkasbaken weather station from the “Southern African Science Service Centre for

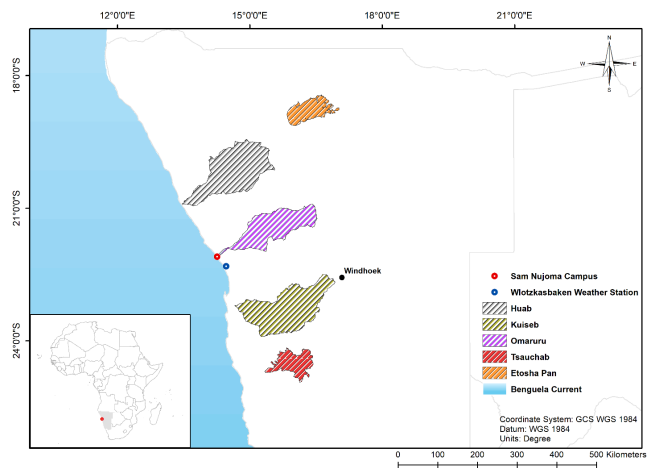


Figure 1: Location of the Sam Nujoma campus, the Wlotzkasbaken weather station, and important Namibian dust sources.



Figure 2: E-samplers (mounted on tripod stands) that were used to concurrently measure $\text{PM}_{2.5}$ (left) and PM_{10} (right).

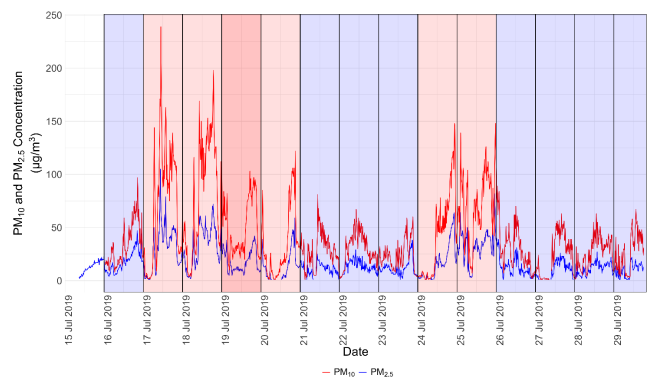


Figure 3: Time series showing the observed $\text{PM}_{2.5}$ (blue) and PM_{10} (red) concentrations ($\mu\text{g}/\text{m}^3$) during the sampling period. The red boxes indicate the days on which HAEs were identified while the blue boxes indicate the LAEs.

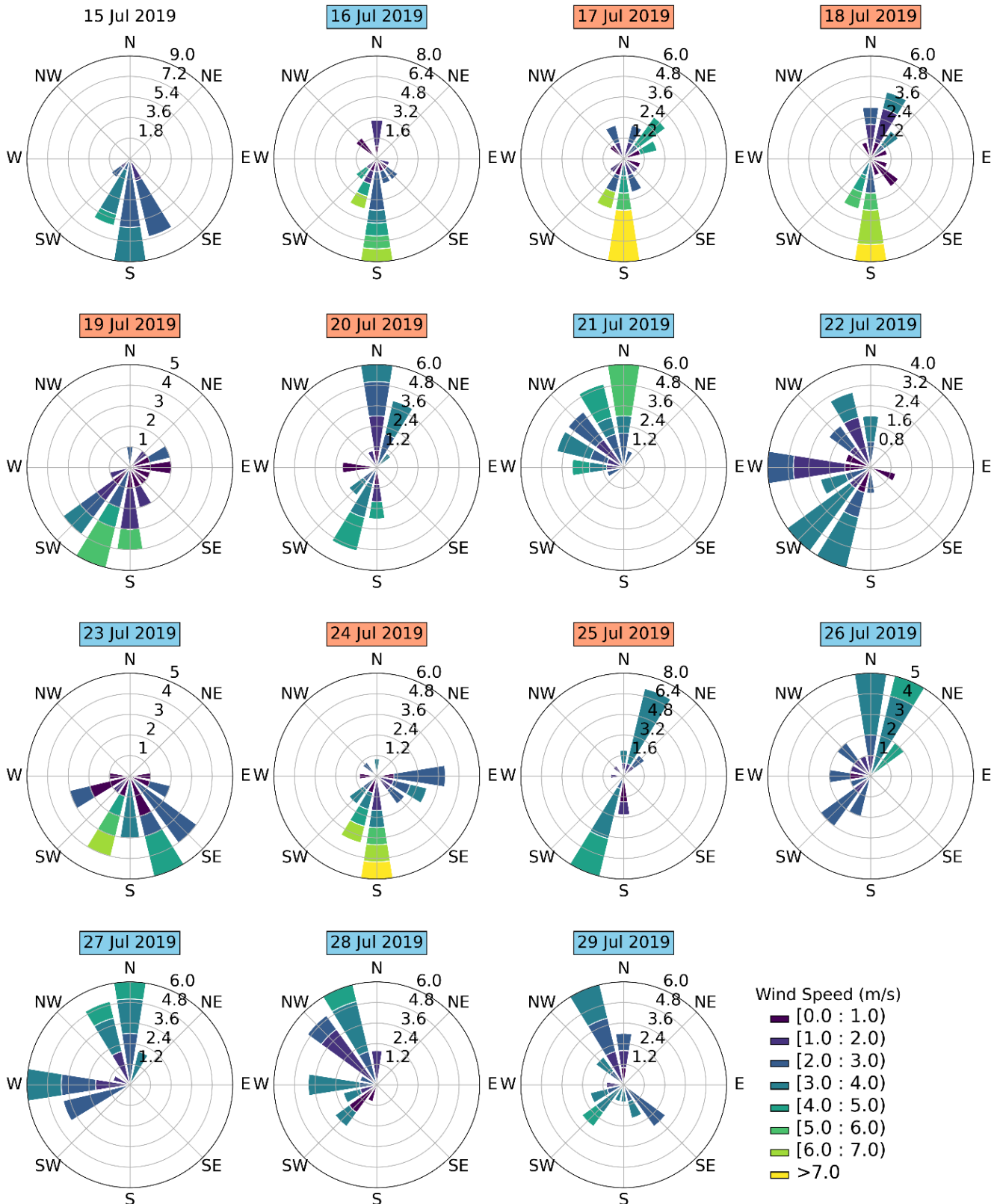


Figure 4: The prevailing daily wind speed and direction at the Sam Nujoma campus during the sampling period. The dates highlighted in red represent the days on which there were HAE events while LAEs are highlighted in blue.

Climate Change and Adaptive Land Management” (SASSCAL) is located about 32 km southeast of the monitoring site (Kaspar et al., 2015). An hourly wind speed and wind direction dataset

for the weather station was obtained from the SASSCAL website, given its proximity to Henties Bay. This dataset was used to create both daily and hourly windroses for the sampling period.

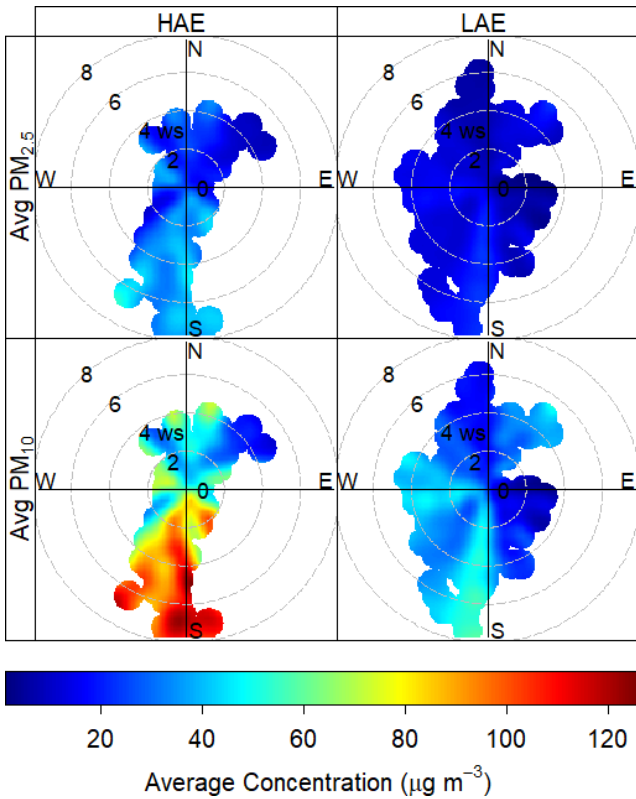


Figure 5: Polar plots illustrating potential $PM_{2.5}$ and PM_{10} emission sources affecting observed concentrations at Henties Bay.

Dust event identification

Presently, there is no clear and agreed-upon method for defining dust events based on PM data (Wiggs et al., 2022). Therefore, in this study, we identified a dust event where the average hourly PM_{10} measurements remained at or above $20.055 \mu\text{g}/\text{m}^3$ for 80% of the day. This concentration represents a “severe dust storm” according to the classification by Leys et al. (2011) and is a very conservative identifier of a dust event. We chose this as the most appropriate classification for this study as the hourly PM_{10} concentrations never reached the thresholds of the other classes. Days which met these criteria were classified as high aerosol episodes (HAEs) while days which did not were classified as low aerosol episodes (LAEs).

HYSPLIT back trajectory analysis

For this study (Stein et al., 2015), the National Oceanic and Atmospheric Administration’s (NOAA) Hybrid Single-Particle Lagrangian Integrated Trajectory (HYSPLIT) model ran 72-hour back-trajectories, which were initiated at a height of 250 m above ground level. The purpose of starting at this height was to model the transport of air masses into the marine boundary layer, which has a minimum height of approximately 500 m over the Namibian region (Klopper et al., 2020). The chosen height of 250 m corresponds to the first and second vertical levels in the model, which are situated at 1000 hPa (around 110 m above mean sea level (masl)) and 975 hPa (roughly 300 masl), respectively. The Global Data Assimilation System (GDAS) reanalysis dataset, which is provided by the National Centre for Environmental Prediction (NCEP) and has a resolution of

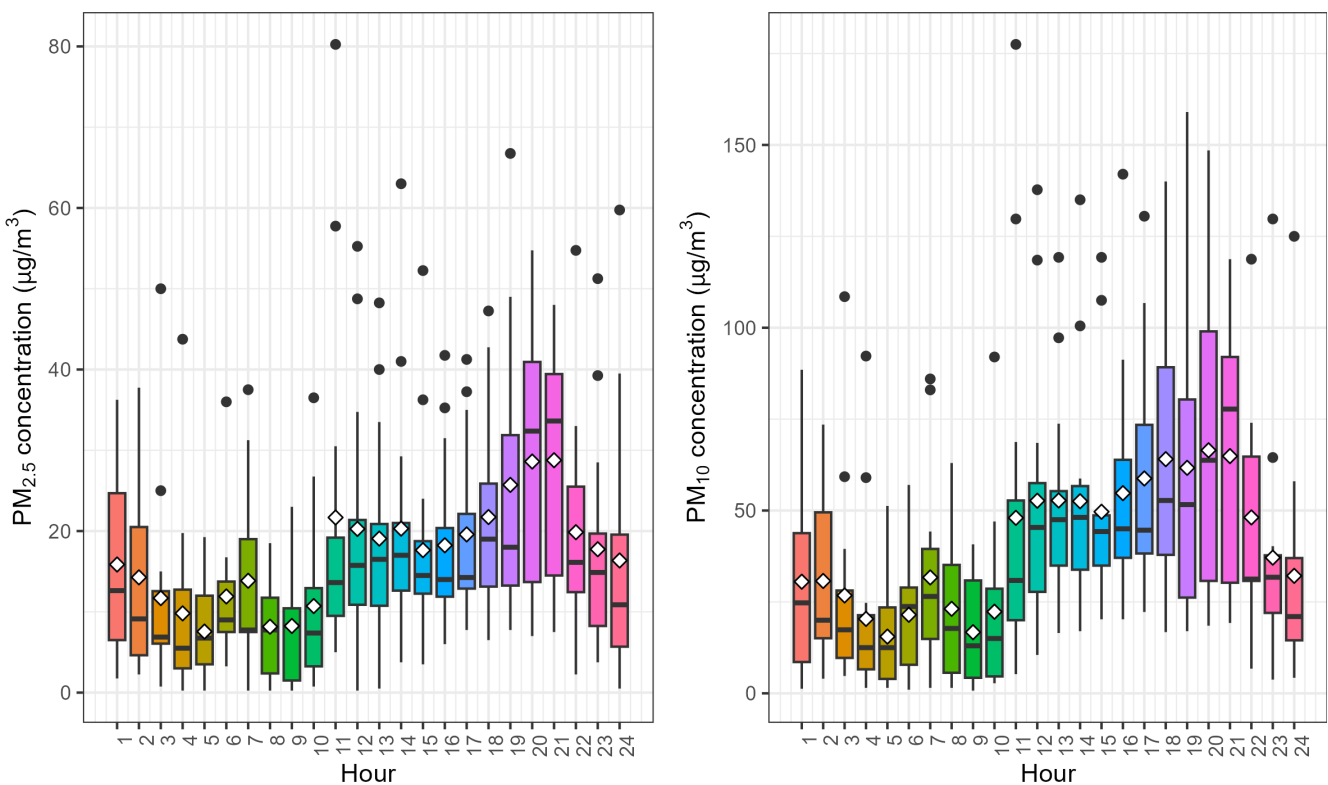


Figure 6: Diurnal variation in $PM_{2.5}$ (left) and PM_{10} (right) concentration ($\mu\text{g}/\text{m}^3$) observed during the sampling period. The white dots indicate the mean while the black dots indicate outliers. Please note that the graphs are on different y-axis scales.

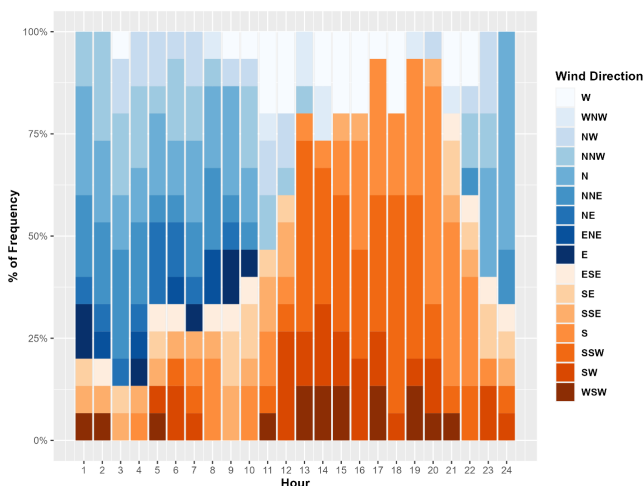


Figure 7: Stacked bar graph illustrating the predominant wind directions per hour.

1°x1°, was used to model these trajectories. The modelling was conducted using the Rstudio interface for Windows and relied on the rich_iannone/splitR and Openair packages from the open-source libraries (splitR is available from <https://github.com/rich-iannone/SplitR>; Carslaw & Ropkins, 2017).

Results and discussion

Daily PM concentrations

Figure 3 shows a time series of the 15-minute PM_{2.5} and PM₁₀ concentrations between 15 and 29 July 2019. The figure also highlights days when HAEs were observed. During the sampling period, the PM_{2.5} concentrations ranged from 1.00–105.00 µg/m³ with a mean value of 17.70 ± 14.38 µg/m³. On the other hand, PM₁₀ concentrations ranged from 1.00–239.00 µg/m³ with a mean value of 41.12 ± 35.31 µg/m³. According to the ‘dust event’ criteria, 17, 18, 19, 20, 24, and 25 July were classified as HAEs and the rest as LAEs. During the HAEs, the mean PM_{2.5} concentration was 24.70 ± 18.20 µg/m³ and the mean PM₁₀ concentration was 57.70 ± 44.20 µg/m³. In contrast, during LAEs, the mean PM_{2.5} and PM₁₀ concentrations were 12.7 ± 7.70 µg/m³ and 28.20 ± 17.80 µg/m³, respectively. The daily windrose plots in Figure 4 provide additional insight into the meteorological factors that may have affected the observed differences in PM_{2.5} and PM₁₀ concentrations during HAEs and LAEs. On days with HAEs, the wind rose plots show predominant southerly and southwesterly winds at speeds exceeding, on most days, 6 m/s. These speeds were the highest during the sampling period and agree with Klopper et al. (2020). Given the location of the study site, of course, the dominant PM source located upwind in those directions is the adjacent ocean. On 20 and 25 July, however, there were winds exceeding 4 m/s from the north and northeast suggesting a second potential emission source.

This is expected as the study by Klopper et al. (2020) showed that aerosol concentrations at the site are influenced mainly by sea salt (74.7%) followed by mineral dust (15.7%), ammonium

Table 1: Summary of the synoptic meteorology during the study period. The days on which there were HAEs are highlighted in yellow.

Date	Episode	Synoptic Condition	Transport Origin
15-16 July	LAE	West coast trough, easterly transport	No long-range transport from further east
17-19 July	HAE	West coast trough, strong pressure gradient	Transport of air from central South Africa, Zimbabwe, Zambia
20-21 July	LAE	West coast trough, strong pressure gradient	Transport of air from central South Africa, Zimbabwe, Zambia
22 July	LAE	High pressure directly over the study site	Very little air transport from the subcontinent
23 July	LAE	Onshore flow along South-Atlantic High	Dominant circulation is driven onshore
24-25 July	HAE	West coast trough, strong pressure gradient	Transport of air from central South Africa, Zimbabwe, Zambia
26 July	LAE	West coast trough, strong pressure gradient	Transport of air from central South Africa, Zimbabwe, Zambia
27-28 July	LAE	Stable weather, no pressure gradient	No pressure gradient near Henties Bay, stable weather

(6.1%), fugitive dust sources (2.6%), and emissions from industry (0.9%). However, on 16 and 22 July, the predominant wind directions were also southwesterly and westerly, during an LAE. This suggests that other factors may also have influenced the observed PM concentrations and subsequent HAEs and LAEs.

For example, PM₁₀ is mostly made up of particles that are directly emitted into the atmosphere (Wong et al., 2022). However, some of its constituents may also be formed through secondary processes. For example, when nitric acid, produced by the oxidation of nitrogen oxides reacts with pre-existing alkaline aerosols like sea salt and dust particles (Bian et al., 2014). According to Klopper et al. (2022), another factor might be present at the synoptic scale. In their study synoptic meteorology was shown to influence the land and sea breezes at the site (Klopper et al., 2020). We created polar plots to examine and display the potential sources of PM_{2.5} and PM₁₀ emissions during HAEs and LAEs (Figure 5). These plots illustrate the variations in PM concentrations based on the wind speeds and directions using polar coordinates, indicating emissions that may affect the receptor site. In addition to the expected dominant contribution of marine sources during HAEs, there appear to be potential continental sources located to the north-northwest and north-northeast of the site. As shown in Figure 1, the Huab riverbed is a potential major source in that direction.

There is also a possible source to the south-southeast and southeast of the site, which may be attributed to contributions from the Kuiseb riverbed. There’s also a contribution around and to the east of the site which is most likely the adjacent Omaruru riverbed.

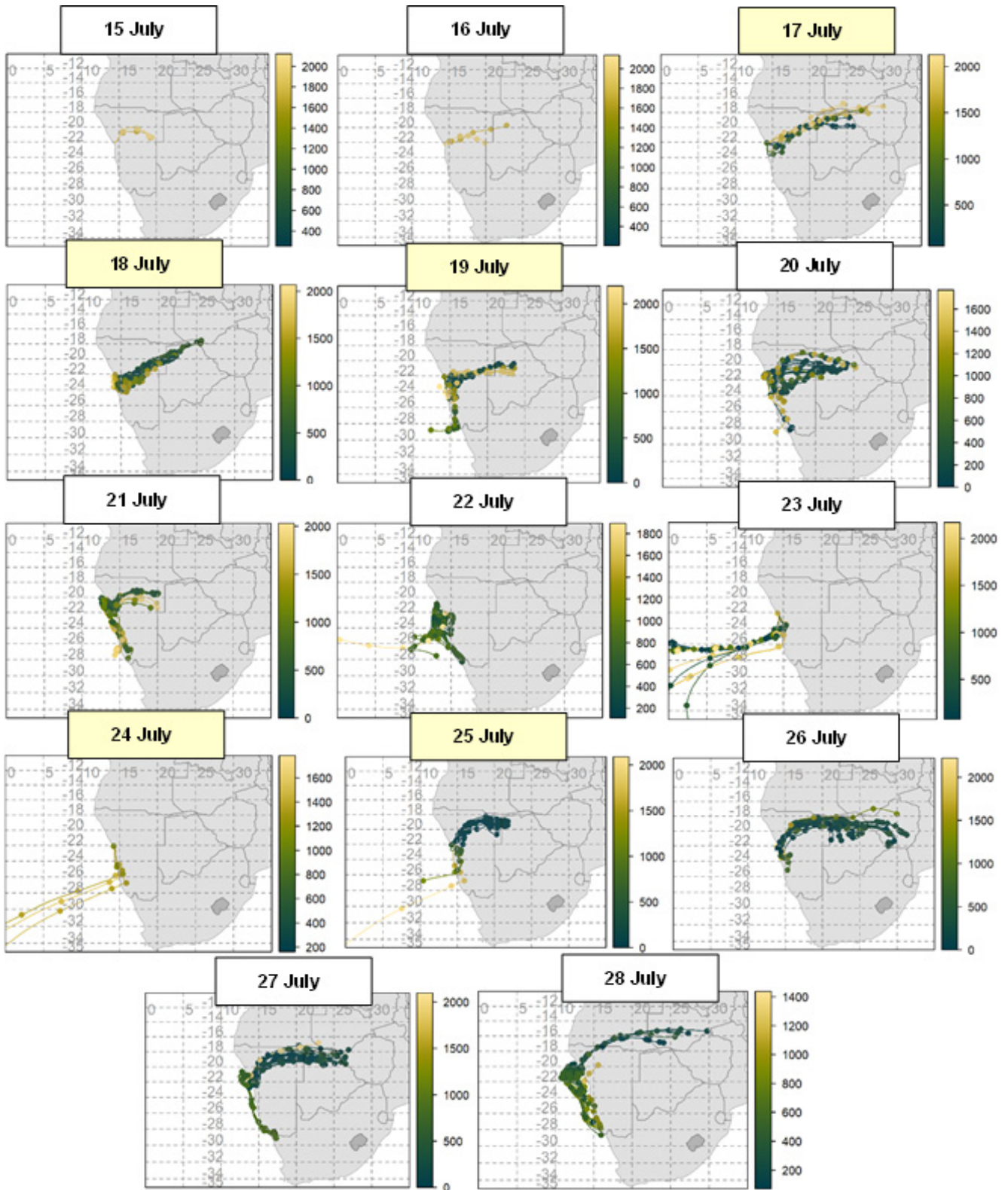


Figure 8: Back-trajectories of 72-hours during 15-28 July 2019 (the different colours indicate the different computed trajectories). The scale to the right indicates the height above ground level (m). The dates on which there were HAEs are highlighted in yellow.

Hourly PM concentrations

The boxplots in Figure 6 show the hourly variation in $PM_{2.5}$ and PM_{10} concentrations over the 2-week sampling period. The plots for both fractions show two clear periods in the diurnal

concentrations. This indicates that the peaks observed in the morning and the beginning of the evening between the two studies are ascribed to different sources. The mean PM concentrations are generally lower during the early morning

hours (01:00–09:00) and then increase throughout the day, reaching their highest values during the late afternoon and evening hours (16:00–21:00). The maxima and minima also show a large range which indicates that there is a lot of variability in the data. Figure 7 shows the predominant hourly wind directions with a clearly defined and very strong day-night signal. During the day, the predominant wind directions were from the south and southwest while at night, northerly and northeasterly winds were predominant. This agrees with the observation by Klopper et al. (2020) in July 2016 at the site. They found that these day and night wind patterns are associated with sea breezes and land breezes, respectively. The high PM concentration from 09:00 to 21:00 may, therefore, be explained by the dominant sea breezes from the south and southwest during this time. This, in other words, signifies the importance of marine sources to HAE in the region.

Back-trajectories and synoptic meteorology

Figure 8 illustrates the 72-hour back-trajectories computed for the sampling period from 15 to 29 July. During most of the study period, air masses were predominantly transported from the interior. During HAEs, air masses were predominantly transported from the northeastern interior with some from the adjacent ocean. During LAEs, the transport was more varied – on some days air masses were transported from the ocean and on other days from the continent. The lowest PM concentrations were observed between 23–24 July (LAE) and during these days, the dominant transport pathway was from the adjacent ocean.

The synoptic conditions during the sampling period are summarised in Table 1. Generally, HAEs occurred under west coast trough conditions, requiring a strong pressure gradient, and enhanced easterly winds from the central regions. The sources of the aerosols might be as far as southern Zambia, the Caprivi, and dry western Namibian regions, as indicated by the back-trajectory. These conditions were also present on July 25 and 26, with transport from as far as central Zimbabwe. Transport during July may coincide with large veld fires over the region, which can explain why circulation with an inland origin is associated with high aerosol concentrations.

Conclusions

This study presents the results of a detailed analysis of daily $PM_{2.5}$ and PM_{10} concentrations between 15 and 29 July 2019 at Henties Bay, Namibia. The results show that during HAEs, the mean $PM_{2.5}$ concentration was $28.40 \pm 18.10 \mu\text{g}/\text{m}^3$ and the mean PM_{10} concentration was $68.20 \pm 44.3 \mu\text{g}/\text{m}^3$. During LAEs, the mean $PM_{2.5}$ and PM_{10} concentrations were $13.3 \pm 9.52 \mu\text{g}/\text{m}^3$ and $30.00 \pm 23.00 \mu\text{g}/\text{m}^3$, respectively. During HAEs, the predominant southerly and southwesterly winds are from the adjacent ocean. The results also show three other sources of PM

emissions to the north and southeast of the site which are most likely the Namibian ephemeral river valleys. Hourly, the highest PM concentrations were observed during the late afternoon and evening hours (16:00–21:00). These concentrations may be explained by the dominant sea breezes from the south and southwest during this time.

During most of the study period, air masses were predominantly transported from the interior. During high aerosol episodes (HAEs), air masses were predominantly transported from the northeastern interior with some from the adjacent ocean while during low aerosol episodes (LAEs), the transport was more varied with air masses being transported from both the ocean and the continent. HAEs generally occurred under west coast trough conditions, requiring a strong pressure gradient and enhanced easterly winds from the central regions. The sources of aerosols might be as far as southern Zambia, the Caprivi, and dry western Namibian regions, as indicated by the back-trajectories. The occurrence of winter veld fires may explain why circulation with an inland origin is associated with HAEs.

Author contributions

MDB, RPB, and SJP: Study conceptualisation.

MDB: Data analysis and drafting of the paper.

DK, BL, and SJP: Methodology.

This manuscript was reviewed by each of the authors listed above.

Acknowledgements

This research was funded by the National Research Foundation of South Africa (Grant: 120764, 106431, 129320, and 114691).

Conflicts of interest

The authors declare that they have no conflicts of interest to disclose, except for RMG, who is an editor-in-chief of the Clean Air Journal. This relationship has been disclosed to the editorial office and all necessary steps have been taken to ensure that the review process was fair and unbiased.

References

- Andreae, M.O., Elbert, W., & de Mora, S.J. 1995, 'Biogenic sulfur emissions and aerosols over the tropical South Atlantic: Atmospheric dimethylsulfide, aerosols and cloud condensation nuclei', *Journal of Geophysical Research* 100:11335-11356. <https://doi.org/10.1029/94JD02828>
- Bian, Q., Huang, X.H.H. & Yu, J.Z. 2014, 'One-year observations of size distribution characteristics of major aerosol constituents at a coastal receptor site in Hong Kong – Part 1:

An earlier version of this paper was presented at the National Association of Clean Air (NACA) Conference in October 2022 and was published in its Proceedings.

- Inorganic ions and oxalate', *Atmospheric Chemistry and Physics*, 14: 9013–9027. <https://doi.org/10.5194/acp-14-9013-2014>
- Carslaw, D. and Ropkins, K. 2017, 'Package "openair": Tools for the Analysis of Air Pollution Data'. <https://davidcarslaw.github.io/openair/> Accessed 20 July 2022.
- Chen, J. and Hoek, G. 2020, 'Long-term exposure to PM and all-cause and cause-specific mortality: A systematic review and meta-analysis', *Environmental International* 143:105974. <https://doi.org/10.1016/j.envint.2020.105974>
- Dai, Q., Bi, X., Liu, B., Li, L., Ding, J., Song, W. et al. 2019, 'A size-resolved chemical mass balance (SR-CMB) approach for source apportionment of ambient particulate matter by single element analysis', *Atmospheric Environment* 197:45–52. <https://doi.org/10.1016/j.atmosenv.2018.10.026>
- Dansie, A.P., Wiggs, G.F.S & Thomas, D.S.G. 2017, 'Iron and nutrient content of wind-erodible sediment in the ephemeral river valleys of Namibia', *Geomorphology* 290:335–346. <https://doi.org/10.1016/j.geomorph.2017.03.016>
- De Leeuw, G., Andreas, E.L., Anguelova, M.D., Fairall, C.W., Lewis, E.R., O'Dowd, C. et al. 2011, 'Production flux of sea spray aerosol', *Reviews of Geophysics* 49(2):RG2001. <https://doi.org/10.1029/2010RG000349>
- Eckardt, F.D and Kuring, N. 2005, 'SeaWiFS identifies dust sources in the Namib Desert', *International Journal of Remote Sensing* 26:4159–4167. <https://doi.org/10.1080/01431160500113112>
- Fuzzi, S., Baltensperger, U., Carslaw, K., Decesari, S., Denier van der Gon, H., Facchini, M.C. et al. 2015, 'Particulate matter, air quality and climate: lessons learned and future needs', *Atmospheric Chemistry and Physics* 15:8217–8299. <https://doi.org/10.5194/acp-15-8217-2015>
- Jacobson, P.J and Jacobson, K.M. 2013, 'Hydrologic controls of physical and ecological processes in Namib Desert ephemeral rivers: Implications for conservation and management', *Journal of Arid Environments* 93:80–93. <https://doi.org/10.1016/j.jaridenv.2012.01.010>
- Jacobson, P.J., Jacobson, K.M., Angermeier, P.L & Cherry, D.S. 2000, 'Hydrologic influences on soil properties along ephemeral rivers in the Namib Desert', *Journal of Arid Environments* 45:21–34. <https://doi.org/10.1006/jare.1999.0619>
- Kaspar, F., Helmschrot, J., Mhanda, A., Butale, M., de Clercq, W., Kanyanga, J.K., Neto, F.O.S. et al. 2015, 'The SASSCAL contribution to climate observation 12:171–177. <https://doi.org/10.5194/asr-12-171-2015>
- Kastury, F., Smith, E. & Juhasz, A.L. 2017, 'A critical review of approaches and limitations of inhalation bioavailability and bioaccessibility of metal(loid)s from ambient particulate matter or dust', *Science of The Total Environment* 574:1054–1074. <http://dx.doi.org/10.1016/j.scitotenv.2016.09.056>
- Kastury, F., Smith, E., Karna, R.R., Scheckel, K.G. & Juhasz, A.L. 2018, 'An inhalation-ingestion bioaccessibility assay (IIBA) for the assessment of exposure to metal(loid)s in PM₁₀', *Science of The Total Environment* 631–632:92–104. <https://doi.org/10.1016/j.scitotenv.2018.02.337>
- Klopper, D., Formenti, P., Namwoonde, A., Cazaunau, M., Chevaillier, S., Feron, A., Gaimoz, C. et al. 2020, 'Chemical composition and source apportionment of atmospheric aerosols on the Namibian coast', *Atmospheric Chemistry and Physics* 20:15811–15833. <https://doi.org/10.5194/acp-20-15811-2020>
- Leys, J.F., Heidenreich, S.K., Strong, C.L, McTainsh, G.H & Quigley, S. 2011, 'PM₁₀ concentrations and mass transport during "Red Dawn" - Sydney 23 September 2009', *AeoRe*, 3:327–342. <https://doi.org/10.1016/j.aeolia.2011.06.003>
- Liu, Y., Zhang, W., Yang, W., Bai, Z. & Zhao, X. 2018, 'Chemical Compositions of PM_{2.5} Emitted from Diesel Trucks and Construction Equipment', *Aerosol Science and Engineering* 2:51–60. <https://doi.org/10.1007/s41810-017-0020-2>
- Mahowald, N.M., Engelstaedter, S., Luo, C, Sealy, A, Artaxo, P, Benitez-Nelson, C., Bonnet, S. et al. 2009, 'Atmospheric Iron Deposition: Global Distribution, Variability, and Human Perturbations', *Annual Review of Marine Science* 1:245–278. <https://doi.org/10.1146/annurev.marine.010908.163727>
- Met One Instrument. 2011, 'E-Sampler-9800 Manual Rev M'. *E-Sampler Particulate Monitor Operation Manual*.
- Piketh, S.J. 2000, 'Transport of Aerosols and Trace Gases over Southern Africa', Johannesburg: University of the Witwatersrand, (Thesis-PhD).
- Poulton, S.W. 2002, 'The low-temperature geochemical cycle of iron: From continental fluxes to marine sediment deposition', *American Journal of Science* 302: 774–805. <https://doi.org/10.2475/ajs.302.9.774>
- Prospero, J.M. 2002, 'Environmental characterisation of global sources of atmospheric soil dust identified with the NIMBUS 7 Total Ozone Mapping Spectrometer (TOMS) absorbing aerosol product', *Reviews of Geophysics* 40:1–31. <https://doi.org/10.1029/2000rg000095>
- Psistaki, K., Achilleos, S., Middleton, N. & Paschalidou, A.K. 2023, 'Exploring the impact of particulate matter on mortality in coastal Mediterranean environments', *Science of The Total Environment* 865:161147. <https://doi.org/10.1016/j.scitotenv.2022.161147>
- Squizzato, S., Cazzaro, M., Innocente, E., Visin, F., Hopke, P.K. & Rampazzo, G. 2017, 'Urban air quality in a mid-size city – PM_{2.5}

composition, sources and identification of impact areas: From local to long range contributions', *Atmospheric Research* 186:51-62. <https://doi.org/10.1016/j.atmosres.2016.11.011>

Stein, A.F., Draxler, R.R., Rolph, G.D., Stunder, B.J.B., Cohen, M.D & Ngan, F. 2015, 'NOAA's HYSPLIT Atmospheric Transport and Dispersion Modeling System', *Bulletin of the American Meteorological Society* 96:2059–2077. <https://doi.org/10.1175/bams-d-14-00110.1>

Vickery, K.J., Eckardt, F.D & Bryant, R.G. 2013, 'A sub-basin scale dust plume source frequency inventory for southern Africa, 2005–2008', *Geophysical Research Letters* 40:5274–5279. <https://doi.org/10.1002/grl.50968>

Wiggs, G.F.S., Baddock, M.C., Thomas, D.S.G., Washington, R., Nield, J.M., Engelstaedter, S. et al. 2022, 'Quantifying Mechanisms of Aeolian Dust Emission: Field Measurements at Etosha Pan, Namibia', *Journal of Geophysical Research: Earth Surface* 127(8):e2022JF006675. <https://doi.org/10.1029/2022jf006675>

Wong, Y.K., Liu, K.M., Yeung, C., Leung, K.K.M. & Yu, J.Z. 2022, 'Measurement report: Characterisation and source apportionment of coarse particulate matter in Hong Kong: insights into the constituents of unidentified mass and source origins in a coastal city in southern China', *Atmospheric Chemistry and Physics* 22: 5017–5031. <https://doi.org/10.5194/acp-22-5017-2022>

Yang, H., Peng, Q., Zhou, J., Song, G. & Gong, X. 2020, 'The unidirectional causality influence of factors on PM_{2.5} in Shenyang city of China', *Scientific Reports* 10:8403. <https://doi.org/10.1038/s41598-020-65391-5>

Zalakeviciute, R., Rybarczyk, Y., Granda-Albuja, M.G., Suarez, M.V.D., & Alexandrino, K. 2020, 'Chemical characterisation of urban PM₁₀ in the Tropical Andes', *Atmospheric Pollution Research* 11:343-356. <https://doi.org/10.1016/j.apr.2019.11.007>